ACS OMEGA

http://pubs.acs.org/journal/acsodf

Article

Integrative Proteome and Ubiquitinome Analyses Reveal the Substrates of BTBD9 and Its Underlying Mechanism in Sleep Regulation

Zhenfei Gao,[#] Anzhao Wang,[#] Yongxu Zhao, Xiaoxu Zhang, Xiangshan Yuan, Niannian Li, Chong Xu, Shenming Wang, Yaxin Zhu, Jingyu Zhu, Jian Guan,* Feng Liu,* and Shankai Yin*

Cite This: *ACS Omega* 2022, 7, 11839−11852

Read Online

ABSTRACT: Ubiquitination is a major posttranslational modification of proteins that affects their stability, and E3 ligases play a key role in ubiquitination by specifically recognizing their substrates. BTBD9, an adaptor of the Cullin-RING ligase complex, is responsible for substrate recognition and is associated with sleep homeostasis. However, the substrates of BTBD9-mediated ubiquitination remain unknown. Here, we generated an SH-SY5Y cell line stably expressing *BTBD9* and performed proteomic analysis combined with ubiquitinome analysis to identify the downstream targets of BTBD9. Through this approach, we identified four potential BTBD9-mediated ubiquitination substrates that are targeted for degradation. Among these candidate substrates, inosine monophosphate dehydrogenase (IMPDH2), a novel target of BTBD9-mediated degradation, is a potential risk gene for sleep dysregulation. In conclusion, these findings not only demonstrate that proteomic analysis can be a useful general approach for the systematic identification of E3 ligase substrates but also identify novel substrates of BTBD9, providing a resource for future studies of sleep regulation mechanisms.

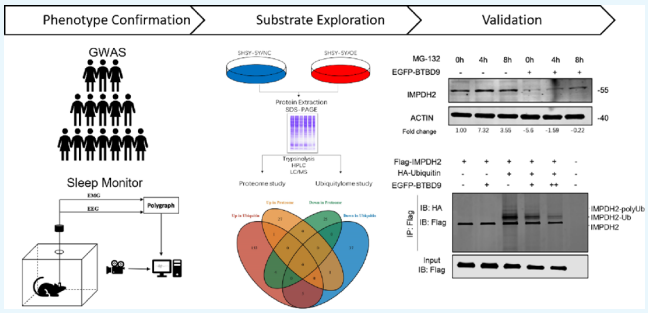

1. INTRODUCTION

Ubiquitination, one of the most important posttranslational modifications of proteins, occurs in all cells and is essential for numerous aspects of cell physiology. In addition, the ubiquitin−proteasome system (UPS) is a common mechanism of protein degradation.[1] In recent years, considerable progress has been made in elucidating the molecular action of ubiquitin in signaling pathways and the mechanism by which the UPS leads to the development of distinct human diseases such as cancer, metabolic syndromes, neurodegenerative diseases, and sleep disorders.[2−4]

Ubiquitin (Ub) is a 76-amino acid protein with seven lysine residues, all of which can be ubiquitinated by a three-enzyme cascade consisting of an E1 Ub-activating enzyme, E2 Ub-conjugating enzyme, and E3 Ub-protein ligase and subsequently attached to a specific substrate to generate different polyubiquitin chains.[5] E3s are the critical components of this cascade because they strictly regulate both the efficiency and substrate specificity of the ubiquitination reaction.[6] Cullin-RING ligase (CRL) complexes are a major group of E3s and are characterized by a RING-finger structure and an adaptor protein that is responsible for substrate recognition.[7] Increasing studies have shown that CRLs play an important role in sleep regulation.[3,8,9]

BTBD9 is a member of the BTB/POZ protein family and serves as an adaptor protein of CULLIN3 (CUL3) to participate in ubiquitination reactions.[10] Genetic studies have found that *BTBD9* gene polymorphisms are important risk factors for sleep disorders.[11,12] In addition, studies using *Btbd9* knockout mice and *dBTBD9* knockout drosophila have confirmed that *BTBD9* is a sleep regulation factor.[13,14] Systematic quantitative proteomic studies have revealed the presence of a stable interaction between BTBD9 and CUL3, but the role of CUL3-mediated ubiquitination in human circadian rhythms and sleep structure is not clear. However, there is sufficient evidence that CUL3 is a crucial component of the Drosophila clock.[15] Overall, these findings suggest that BTBD9 may regulate sleep or wakefulness through CUL3-mediated protein ubiquitination. However, the downstream substrate that is ubiquitinated via the interaction between BTBD9 and CUL3 to influence sleep regulation remains unknown, and the mechanisms by which BTBD9 and CUL3 exert their effects also need to be further studied.

Received: December 23, 2021
Accepted: March 24, 2022
Published: March 31, 2022

https://doi.org/10.1021/acsomega.1c07262
ACS Omega 2022, 7, 11839−11852

To identify the specific substrates of BTBD9-mediated ubiquitination, we generated SH-SY5Y cell lines stably expressing *BTBD9* and performed proteomic and ubiquitinome analyses. Ubiquitinome analysis revealed that BTBD9 significantly contributes to the overall protein ubiquitination state and suggested a potential role for BTBD9 in regulating protein localization and neurodegenerative diseases. Ubiquitinome analysis in combination with quantitative proteomic analysis showed that the levels of four candidate substrates are decreased, with IMPDH2 showing the most significant change in expression. We further validated that the ubiquitination of IMPDH2 is mediated by BTBD9 and identified IMPDH2 as a novel sleep dysregulation risk gene. This is the first study to systematically explore the substrates of BTBD9 and its combined effects on the substrate proteins. We believe that this study may help us reveal the mechanisms by which *BTBD9* affects sleep and provide new ideas for sleep regulation.

2. MATERIALS AND METHODS

2.1. Sleep Parameters Recording of Btbd9$^{PB/PB}$ Mice. *2.1.1. Animals.* The specific pathogen-free (SPF) C57BL/6 J male wild-type (WT) mice (2 months old, 18−20 g) were purchased from Shanghai Laboratory Animal Center, Chinese Academy of Science (SLAC, Shanghai, China), and *Btbd9$^{PB/PB}$* mice were kindly gifted from Prof. Wu Xiaohui (Fudan University) and housed four to five per cage under a constant temperature (22 ± 0.5 °C), humidity (55 ± 5%), and an automatically controlled 12 h light/12 h dark cycle (lights on at 7 a.m.), with access to food and water ad libitum. The study protocol was approved by the Institutional Animal Care and Use Committee of Shanghai Jiao Tong University Affiliated Sixth People's Hospital (no. 2021-0149).

2.1.2. EEG/EMG Recording Electrode Implantation. Mice were first anesthetized with a 2−3% isoflurane/oxygen mixture. After completion of scalp preparation and sterilization, the mice's heads were fixed on a stereotaxic holder and two small holes (1 mm in diameter) were drilled in the frontal (AP/ML: +1.50/−0.80 mm) and parietal (AP/ML: −1.50/−1.00 mm) bone surfaces to facilitate the implantation procedure. During surgery, the EEG electrodes were screwed into the bone holes in the frontal and parietal lobes, while the EMG electrodes were inserted into the bilateral oblique muscles. Subsequently, the EEG and EMG electrodes were attached to a miniature connector to form an electrode assembly, which was then fixed to the skull surface with tooth-based acrylic resin. After the surgical mice were housed individually and recovered for 7 days, monitoring of video polysomnography recordings was carried out.

2.1.3. Video-Polysomnography Recordings and Data Analysis. Video PSG recordings were performed as previously described.[16] Briefly, mice were connected to the device and habituated for 3 days prior to formal recording. Cortical EEG and cervical EMG signals were digitized at a sampling rate of 512 Hz, amplified, filtered (Biotex), and then recorded through a CED 1401 digitizer and Spike 2 software (CED, UK). The Spike 2 data were then converted to appreciable vigilance states using SleepSign software (Kissei Comtec, Japan). By this method, the alertness states of the mice (scored every 4 s timing) were automatically classified as wake, rapid eye movement sleep (REM), and non-rapid eye movement sleep (NREM). The sleep classification was then manually checked and corrected in case of incompatibility. After manual calibration and correction, the number, percentage, transition, and duration of each alert state were calculated.

2.2. Cell Culture and Transfection. SH-SY5y cells were kindly provided by the Stem Cell Bank, Chinese Academy of Sciences and cultured in Dulbecco's modified Eagle's medium (DMEM) plus 10% fetal bovine serum and penicillin and streptomycin at 37 °C in 5% CO_2 (v/v). Cells were seeded in a six-well plate and grown to 70−90% confluent for transfection. For each well, 1 μg of the plasmid and 2 μL of the Lipofectamine 2000 reagent were mixed in an Opti-MEM medium and incubated for 25 min at room temperature. The mixture was added to a cell culture medium in the absence of serum for 6 h and then changed to complete the medium.

2.3. Real-Time qPCR. Total RNA was extracted from cells using an EZ-press RNA purification kit (EZBioscience, MN, USA), and EZ-press reverse transcriptase kits were used to synthesize cDNA as the template for qPCR with 1 μg of total RNA. All operations were performed in accordance with product instruction.

Relative quantitative analysis of the gene expression level was performed in LightCycler 480 II (ROCHE, USA) according to the operating manual. The thermocycling procedure was set according to the instruction of a Power SYBR Green PCR master mix (2×) provided by EZBioscience. Housekeeping gene *ACTIN* was set as an IC (internal control), and each assay was independently repeated three times. The primers of *BTBD9* and *ACTIN* were listed below:

ACTIN-F:5′-CATGTACGTTGCTATCCAGGC-3′
ACTIN-R:5′-CTCCTTAATGTCACGCACGAT-3′
BTBD9-F:5′-GGCAACGCTGACAGATGAGAA-3′
BTBD9-R:5′-AGGTAGAATCCTCTAGCTCTGGA-3′

2.4. Sample Preparation and MS Data Analysis. The cells were washed with cold 1× PBS twice before being collected from the dishes by trypsin. They were then transferred to a new precooled tube, and liquid nitrogen was added to fully grind the cells into a powder. The samples of each group were added to 4 times the volume of powdered lysis buffer (8 M urea, 1% "Protease Inhibitor Cocktail Set I", 50 μM 3,5-dithiocyanato-pyridine-2,6-diamine; the protease inhibitor was purchased from Merck Millipore (56500)) and lysed by ultrasonication. The samples were first centrifuged at 12,000*g* for 10 min at 4 °C to remove cell debris. Then, the supernatant was transferred to a new centrifuge tube, and the protein concentration was determined using a BCA kit following the manufacturer's instructions.

The protein concentration of each sample protein was adjusted to be the same, and then, the equal volume of these was used for enzymatic hydrolysis and subsequent analysis. Then, 20% trichloroacetic acid (TCA) was slowly added, vortexed, and allowed to settle at 4 °C for 2 h. The samples were centrifuged at 4500*g* for 5 min, and after removing the supernatant, the precipitate was washed two to three times with precooled acetone. After drying the pellet, TEAB was added to a final concentration of 200 mM, the pellet was ultrasonically dispersed, trypsin was added to digest the protein, and the mixture was hydrolyzed overnight. Dithiothreitol (DTT) was added to a final concentration of 5 mM and reduced at 56 °C for 30 min. Then, iodoacetamide (IAA) was added to a final concentration of 11 mM and incubated for 15 min at room temperature in the dark.

The peptides were dissolved in mobile phase A of liquid chromatography and then separated using an EASY-nLC 1200

https://doi.org/10.1021/acsomega.1c07262
ACS Omega 2022, 7, 11839−11852

ultrahigh-performance liquid system. Mobile phase A was an aqueous solution containing 0.1% formic acid and 2% acetonitrile; mobile phase B was an aqueous solution containing 0.1% formic acid and 90% acetonitrile. Liquid gradient setting: 0−62 min, 4−23% B; 62−82 min, 23−35% B; 82−86 min, 35−80% B; 86−90 min, 80% B. The flow rate was maintained at 500 nL/min. The peptides were separated by an ultrahigh-performance liquid system, injected into the NSI ion source for ionization, and then analyzed by Q Exactive HF-X mass spectrometry. The ion source voltage was set to 2.1 kV, and the peptide precursor ions and their secondary fragments were detected and analyzed by a high-resolution Orbitrap. The scanning range of the primary mass spectrum was set to 400−1500 m/z, and the scanning resolution was set to 120,000; the scanning range of the secondary mass spectrum was set to a fixed starting point of 100 m/z, and the secondary scanning resolution was set to 15,000. A data-dependent scanning (DDA) program was used to acquire the mass spectrum data, and after the first level scan, the first 10 peptide precursor ions with the highest signal intensity were selected to enter the HCD collision cell, and 28% of the fragmentation energy was used for fragmentation grade mass spectrometry analysis. To improve the effection of the mass spectrometer, the automatic gain control (AGC) was set to 5×10^4, the signal threshold was set to 2.5×10^5 ions/s, the maximum injection time was set to 40 ms, and the dynamic rejection time of the tandem mass spectrometry scan was set to 30 s to avoid repeated scanning of ions.

2.5. Bioinformatic Analysis. *2.5.1. Enrichment of Gene Ontology Analysis.* Proteins were classified by GO annotation into three categories: the biological process, cellular compartment, and molecular function according to the Gene Ontology database.[17] For each category, a two-tailed Fisher's exact test was employed to test the enrichment of the differentially expressed protein against all identified proteins. The GO with a corrected p value <0.05 is considered significant.

2.5.2. Enrichment of Pathway Analysis. The Encyclopedia of Genes and Genomes (KEGG) database (http://www.kegg.jp/)[18] was used to identify enriched pathways by a two-tailed Fisher's exact test to test the enrichment of the differentially expressed protein against all identified proteins. The pathway with a corrected p value <0.05 was considered significant. These pathways were classified into hierarchical categories according to the KEGG website.

2.5.3. Enrichment of Protein Domain Analysis. For each category proteins, the InterPro database[19] was researched and a two-tailed Fisher's exact test was employed to test the enrichment of the differentially expressed protein against all identified proteins. Protein domains with a corrected p value <0.05 were considered significant.

Over representation analysis was conducted by "clusterProfiler" R packages,[20] and gene set enrichment analysis was performed by GSEA_4.1.0 application.[21]

2.6. Immunoprecipitation (IP). Cells were washed with cold PBS twice and lysed in chilled lysis buffer supplemented with a protease inhibitor mixture. They were then incubated on ice for 30 min. The cell debris was removed after centrifuging at 14,000 rpm for 25 min. The supernatant was subjected to IP with 20 μL of anti-FLAG M2 affinity resin (Sigma) overnight at 4 °C. Resin-containing immune complexes were washed with ice-cold lysis buffer followed by TBS washes. After that, 50 μL of SDS-PAGE sample loading buffer (2×) was added and it was heated at 95 °C for 10 min to denature proteins.

2.7. Western Blots. Total proteins were separated by SDS-PAGE (sodium dodecyl sulfate polyacrylamide gel electrophoresis) and transferred onto PVDF (polyvinylidene fluoride) membranes. Membranes were blocked in 5% non-fat milk diluted in TBS for 1 h and then were incubated with the primary antibody diluted in TBST overnight at 4 °C. Membranes were subsequently incubated with the secondary antibody for 1 h in room temperature after washing with 1× TBS three times. The signals of the proteins were visualized on LI-COR Odyssey (Lincoln, NE, USA). The following antibodies were used: the anti-IMPDH2 antibody (1:2000, Abcam, ab131158), BTBD9 Rabbit poly antibody (1:2000, Abclonal, A18528), anti-FLAG antibody (1:2000, Sigma, F1804), anti-HA antibody (1:2000, Cell Signaling Technology, C29F4), anti-β-actin antibody (1:10000, Abclonal, A2319), anti-GAPDH antibody (1:10000, Abclonal, AC002), anti-Mouse IgG H&L (1:10000, Abcam, ab216778), and anti-Rabbit IgG H&L (1:10000, Abcam, ab216776).

2.8. Genome-Wide Association Studies (GWAS). *2.8.1. Participants.* This GWAS study was performed in the sleep center of Shanghai Jiao Tong University Affiliated Sixth People's Hospital from January 2011 to June 2019 (ongoing SSHS study) according to the Declaration of Helsinki (registration number: ChiCTR1900025714). A written informed consent was obtained from each participant. A total of 725 people were recruited in this study. All participants were asked to complete a uniform questionnaire regarding personal characteristics such as weight, height, and medical histories. Exclusion criteria were as follows: (i) age less than 18 years old; (ii) history of sleep disorders; (iii) psychiatric disturbances, chronic liver disease, or chronic kidney disease; and (iv) unavailable clinical data.

2.8.2. Sleep Parameter Recording. Overnight polysomnography (PSG) monitors were performed in the sleep center of Shanghai Jiao Tong University Affiliated Sixth People's Hospital with an Alice 4 system (Philips Respironics Inc., Pittsburgh, PA, USA). Sleep parameters were obtained from the electroencephalography (EEG) result recorded by PSG including N1 sleep (N1), N2 sleep (N2), N3 sleep (N3), rapid eye movement sleep (REM), wake time (WK), total sleep time (TST), and sleep period time (SPT). The ratio of N1/TST, N2/TST, N3/TST, REM/TST, WK/SPT, and sleep efficiency (SE, TST/SPT) as well as TST was calculated to do the analysis.

2.8.3. Genotyping. Genomic DNA was extracted from the whole blood by a DNA isolation kit (Qiagen). An Affymetrix Genome-Wide Human SNP Array 6.0 (SNP6.0) and Affymetrix Axiom Genome-Wide CHB Array (CHB) were used to detect the specific base sequence of each participant.[22] Data from Affymetrix chips were analyzed by using Genotyping Console version 3.1 software (Affymetrix). Data with a high missing gene call rate (>5%), low MAF (<0.01), and significant deviation from Hardy−Weinberg equilibrium ($P < 1 \times 10^{-6}$) were excluded from analysis.

2.9. Statistic. For comparisons between two groups, Student's t test was used and a p value of <0.05 was considered statistically significant.

3. RESULTS

3.1. Mutations in BTBD9 Cause Sleep Disturbance. To validate the association of *BTBD9* SNPs with sleep architecture, we performed a small-scale GWAS consisting of 785 individuals with standard PSG monitoring. According to the result of this analysis, we drew a Manhattan plot[23,24] and found that there was

https://doi.org/10.1021/acsomega.1c07262
ACS Omega 2022, 7, 11839−11852

a statistically significant association between the intronic *BTBD9* gene variant rs201664431 (GACA > G) and the wake/sleep time (WK/SPT) (Figure 1A). We then compared

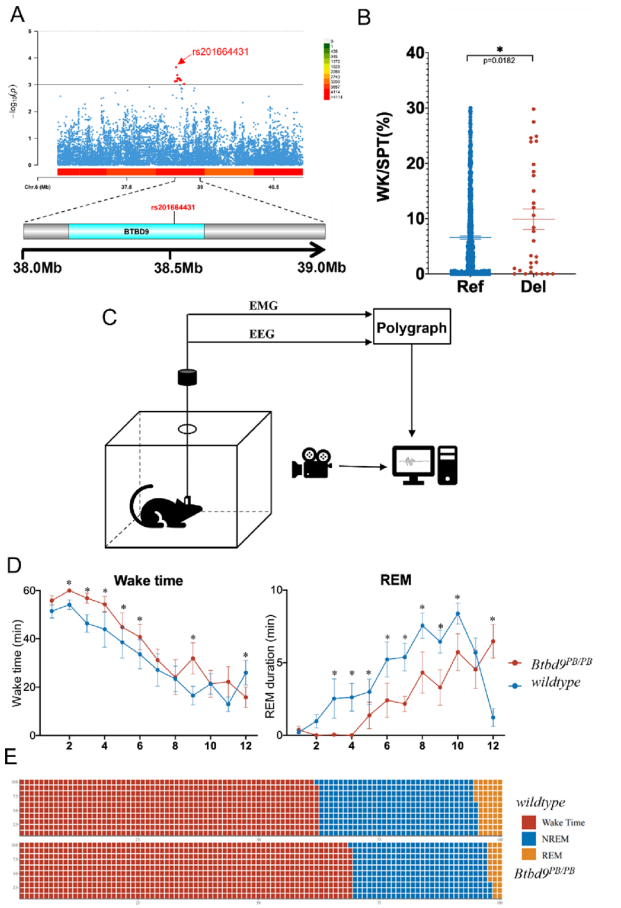

Figure 1. Alteration in *BTBD9* causes sleep disturbance. (A) Manhattan plot showing the distribution of SNPs associated with WK/SPT in people ($p < 10^{-3}$). (B) Comparison of WT/SPT between different phenotypes of rs201664431 by the *t* test (*$p < 0.05$, $n = 725$). (C) Diagram for mouse EEG recording. (D) Line chart that displays the duration of wake time and REM sleep of mice during the night (1 = 19 p.m., 12 = 7 a.m., $n = 3$ in each group, error bar: mean ± SEM, *$p < 0.05$). (E) Average percent of the distinct sleep status of mice during the recording time (7 p.m. to 7 a.m.).

WK/SPT data between individuals of different rs201664431 genotypes, and the results showed that individuals with deletion alleles had longer wake durations than those with reference alleles (Figure 1B).

To better characterize the functional role of *BTBD9* in sleep regulation, a mouse strain with PiggyBac transposase-mediated gene silencing (the *Btbd9*$^{PB/PB}$ strain) was used in this study. Homozygous mice were able to be born, grown to adults, and did not exhibit any apparent abnormalities. The sleep of three pairs of congenic mice was monitored by EEG (Figure 1C). Each of the mice underwent recording for 3 days to obtain stable data. We separated the sleep/wake statuses of the mice into three categories: WAKE, REM sleep, and NREM sleep. By comparing the duration that the mice spent in each status, we found that, from 7 p.m. to 7 a.m., the WAKE durations of the *Btbd9*$^{PB/PB}$ mice were significantly longer than those of the wild-type controls, while the REM sleep durations of the *Btbd9*$^{PB/PB}$ mice were significantly shorter than those of the wild-type controls (Figure 1D). Accordingly, analysis of the average durations of wake time and REM sleep from 7 p.m. to 7 a.m. showed a similar result (Figure 1E).

Taken together, these data confirmed that *BTBD9* plays a crucial role in sleep regulation.

3.2. Ubiquitinome Profiling of BTBD9 Overexpression Cells. To systematically analyze the global change in the ubiquitylated targets of BTBD9 and identify its specific substrate, we carried out quantitative proteomic and ubiquitinome profiling of *BTBD9* overexpression (OE) cells (Figure 2A). OE cells were generated using neuroblastoma SH-SY5Y cells, which are commonly used for neuroscience research, because of their human origin, catecholaminergic neuronal properties, and ease of maintenance.[25] Cells stably transfected with an empty vector were used as negative controls (NC). The efficiency of OE was validated by quantitative RT-PCR (qRT-PCR) and western blotting (Figure 2B). To ensure data reproducibility, proteins were extracted from three biological replicates of each cell line. Correlation analysis showed that the correlation coefficient between the two groups was greater than 0.9, indicating good reproducibility (Figure 2C).

Ubiquitinome profiling identified 8411 ubiquitylated lysine residues in 2947 proteins, and of 5973 of these ubiquitylated lysine residues, 1738 proteins were found in both the NC and OE groups. The ubiquitylation of 216 lysine residues in 163 proteins was significantly increased after *BTBD9* overexpression, and the ubiquitylation of 43 lysine residues in 43 proteins was significantly decreased when using a fold change = 1.5 and *p* value <0.05 as thresholds to define differentially modified targets (Figure 2D). The global ubiquitination level was significantly elevated in SH-SY5Y cells by *BTBD9* overexpression since there were many more targets that showed increased ubiquitylation than targets that showed decreased ubiquitylation (Figure 2E,F); this finding is consistent with the previously characterized biological functions of BTBD9.[10] Furthermore, five proteins contained both residues that showed increased ubiquitylation and residues that showed decreased ubiquitylation (Figure 2G). TNFAIP1 is a previously identified substrate of BTBD9-mediated ubiquitination and is degraded by the proteasome.[26] In our study, although TNFAIP1 was not identified as a significantly differentially modified protein because it was only detected in one sample in each group, the level of TNFAIP1 in these two samples suggested that the ubiquitination of TNFAIP1 was strongly promoted by BTBD9.

To better understand the preference of enzymes for substrates, we analyzed the sequence motifs of ubiquitylated peptides in OE and NC cells with the motif-x algorithm.[27] The result shows that 20 amino acid residues, from upstream 10 amino acid sites to the downstream 10 amino sites, around the differential modified lysine sites could be categorized into 10 motifs. These motifs are KL, IxK, DK, LK, LxK, VxK, DxK, KxxxV, AxK, and NxK (K is the ubiquitylated lysine, and X represents a random amino acid residue) (Figure 3A). Analysis of these motifs suggested that six amino acids were enriched in the motifs including four nonpolar aliphatic amino acids (leucine, isoleucine, alanine, and valine), an acidic amino acid (aspartic acid), and an amide amino acid (asparagine). Furthermore, there was little enrichment of positively charged amino acid residues, suggesting that BTBD9-mediated protein ubiquitination may not be involved in the interaction of proteins with nuclear acids or phospholipids but mainly participates in protein interactions through the hydrophobic interface formed by motifs of BTBD9 targets and their counterparts.

https://doi.org/10.1021/acsomega.1c07262
ACS Omega 2022, 7, 11839−11852

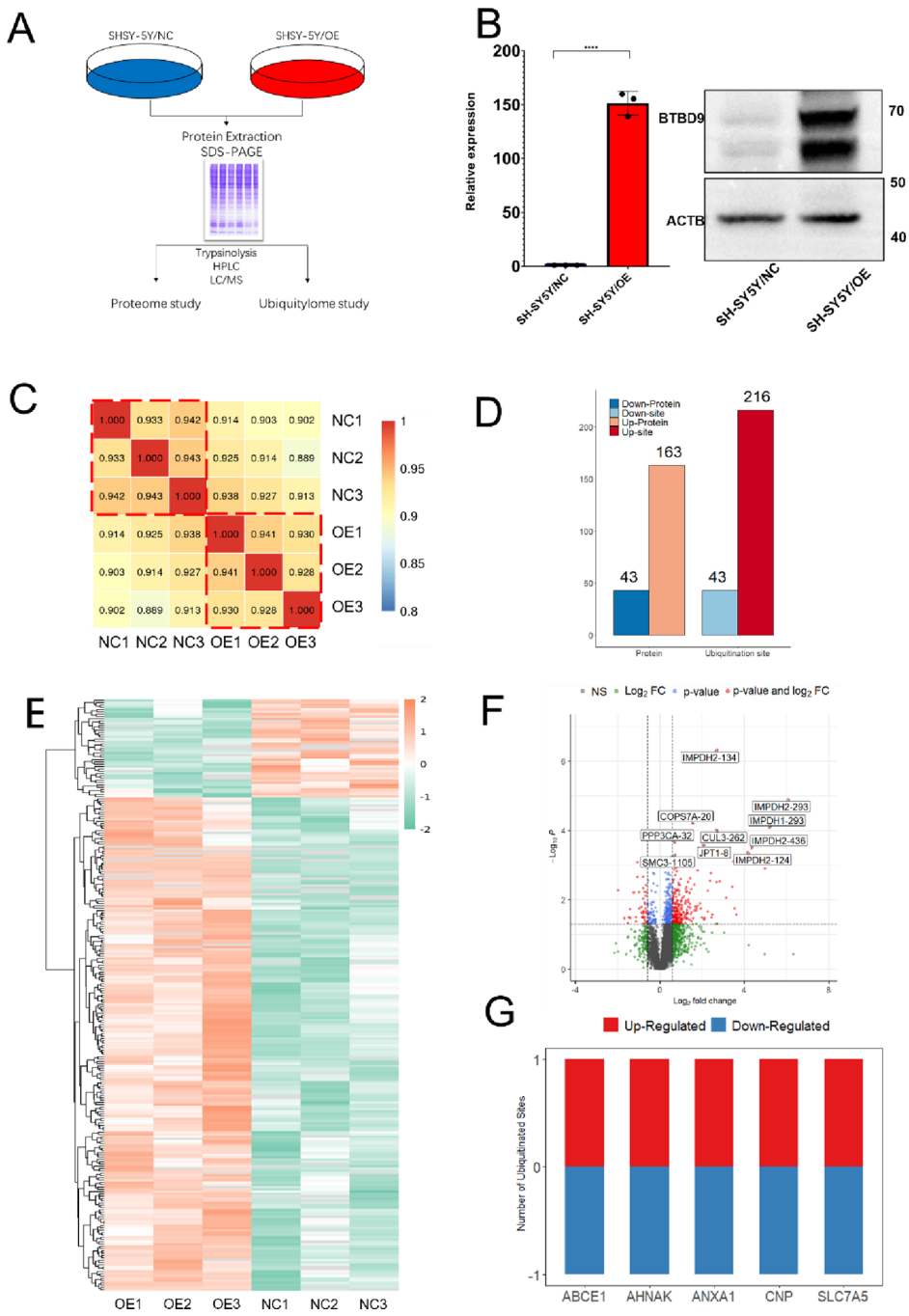

Figure 2. Characterization of protein ubiquitinome in the *BTBD9*-overexpression cell line. (A) Proteome and ubiquitinome project workflow. (B) Validation of BTBD9 overexpression cell line construction by qPCR (t test, ****$p < 0.0001$, $n = 3$ in each group). (C) Correlation analysis of samples within two groups in the ubiquitinome project. (D) Statistic of differential modified lysines and proteins in ubiquitinome. (E) Heatmap displaying differential ubiquitinated proteins. (F) Volcano plot of differential ubiquitinated proteins. (The top 10 were labeled-ordered by the p value). (G) Bar plot showing proteins containing both up- and down-regulated ubiquitylation sites.

3.3. Functional Annotation and Pathway Enrichment Analysis of Differentially Modified Proteins. To understand the biological functions or signaling pathways associated with the ubiquitinylated proteins regulated by BTBD9, gene ontology (GO) enrichment analysis and KEGG pathway analysis were performed. GO enrichment analysis revealed that the proteins that showed increased ubiquitylation after *BTBD9* overexpression were enriched for biological processes associated with "cellular localization", "protein localization", and "nitrogen compound transport" (Figure 3B). Further analysis of the protein interaction network of the enrichment pathways revealed that most of the differentially modified proteins were associated with "cellular localization" and "establishment of localization in cell" (Figure 3C), and these two pathways were the key nodes of the protein interaction network (Figure 3D). In addition, KEGG pathway analysis showed that the proteins that showed increased ubiquitylation were significantly enriched in 14 pathways (Figure 3E), including "amyotrophic lateral sclerosis", "Huntington's disease", and "Parkinson's disease", indicating a potential role for BTBD9-mediated ubiquitination

https://doi.org/10.1021/acsomega.1c07262
ACS Omega 2022, 7, 11839−11852

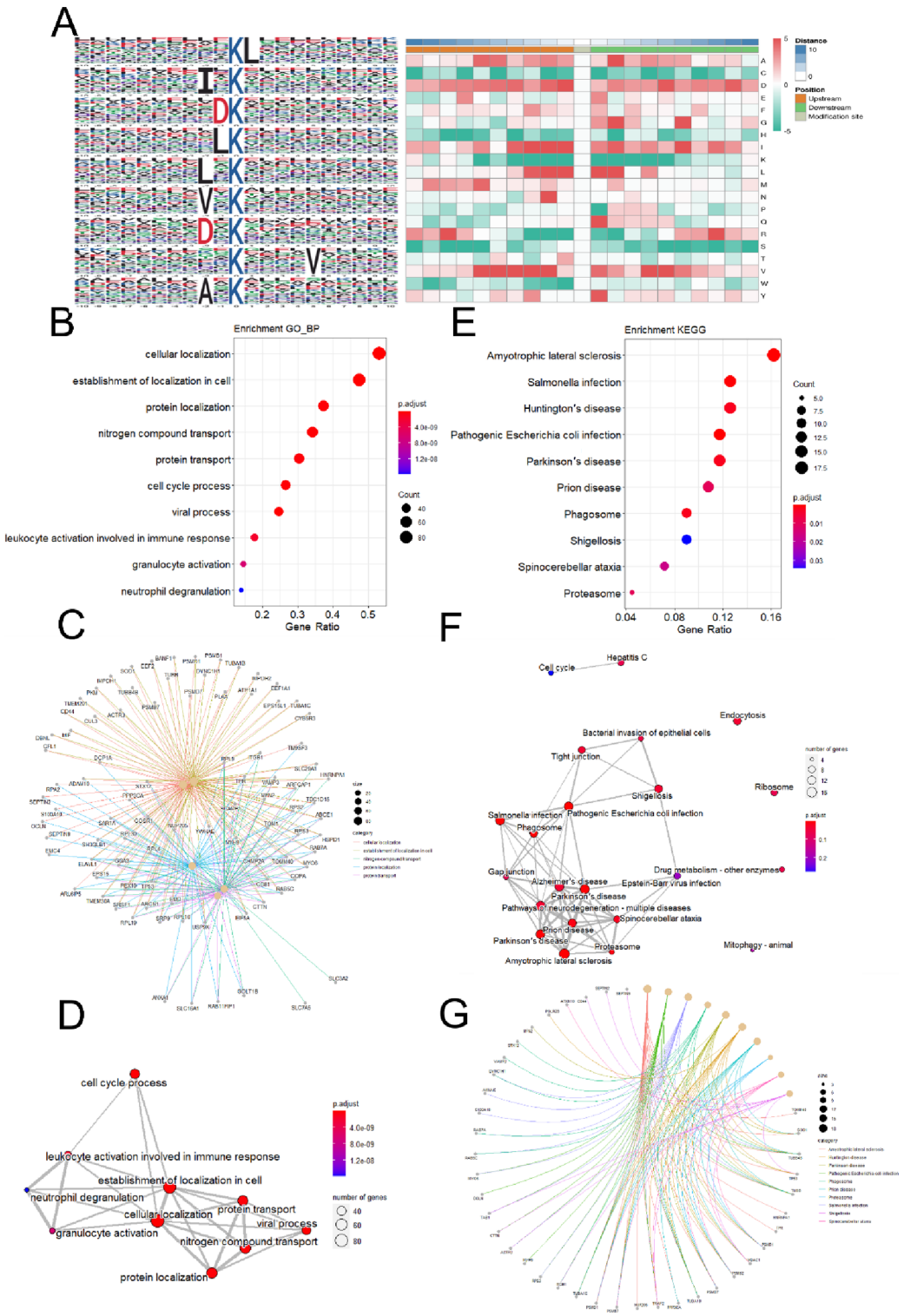

Figure 3. Bioinformatic analysis of ubiquitinome. (A) Ubiquitylation motif diagram and heatmap indicating ubiquitination preference of BTBD9 by analyzing the frequency of the amino acid residues surrounding differential ubiquitylated lysines in each motif. (B) Enrichment analysis of proteins containing up-regulated ubiquitylation sites based on the biological process by Gene Ontology. (C) Diagram showing the top five items of the biological process enriched by proteins containing up-regulated ubiquitylation sites. (D) GO item interaction network of up-regulated ubiquitinated proteins. (E) KEGG pathway analysis of proteins containing up-regulated ubiquitylation sites. (F) Pathway interaction network of up-regulated ubiquitinated proteins. (G) Circular network diagram showing the top 10 items of the KEGG pathway enriched by proteins containing up-regulated ubiquitylation sites.

in the regulation of neurodegenerative diseases. Furthermore, these pathways formed the majority of the pathway interaction network (Figure 3F). Interestingly, most of the enriched signaling pathways were associated with the same proteins, such as the tumor suppressors p53 and β-tubulin (Figure 3G), suggesting that these two proteins are potential targets of

https://doi.org/10.1021/acsomega.1c07262
ACS Omega 2022, 7, 11839−11852

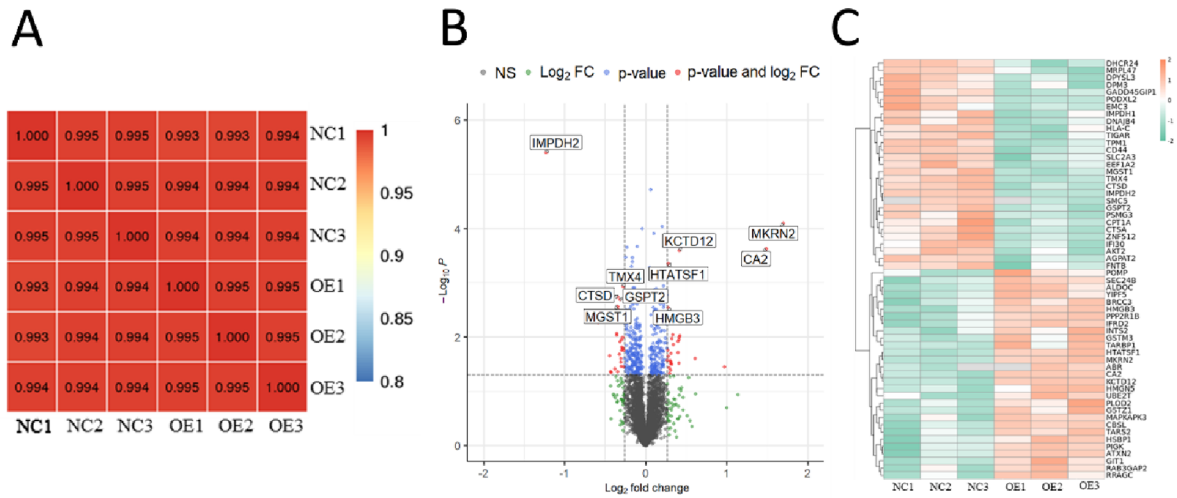

D

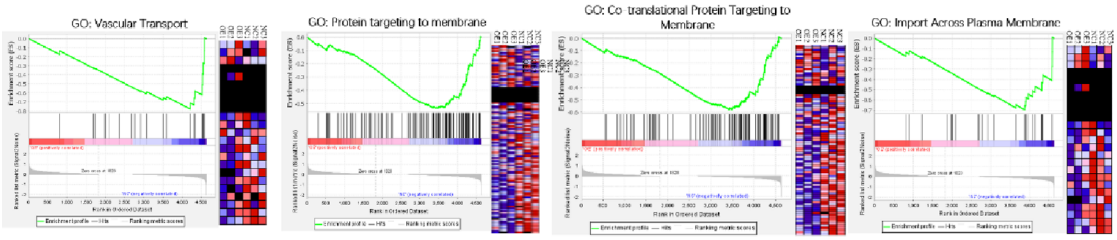

NAME	NES	p-value	FDR
Protein K63 linked ubiquitination	1.94	0.000	0.132
Vascular Transport	-1.99	0.000	0.044
Co-translational Protein Targeting to Membrane	-1.96	0.000	0.052
Protein Targeting to Membrane	-1.92	0.000	0.074
Import Across Plasma Membrane	-1.83	0.000	0.235

E

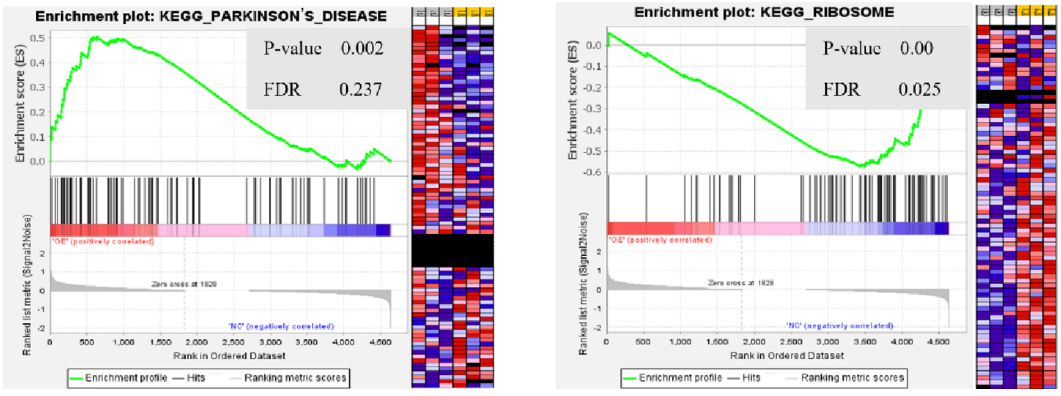

Figure 4. Bioinformatic analysis of proteome. (A) Correlation analysis of samples within two groups in the proteome project. (B) Differential expressed proteins are shown in the volcano plot. (C) Heatmap displaying the differential expressed proteins. (D) GSEA of the biological process of proteome results with the table showing the NES, *p* value, and FDR of each item. (E) GSEA of the KEGG pathway of the proteome result.

BTBD9 and that BTBD9 may potentially regulate tumor progression and the microtubular cytoskeleton.[28,29]

3.4. Proteomic Profiling of BTBD9 Overexpression Cells.

Before we performed quantitative proteomic analysis of

https://doi.org/10.1021/acsomega.1c07262
ACS Omega 2022, 7, 11839−11852

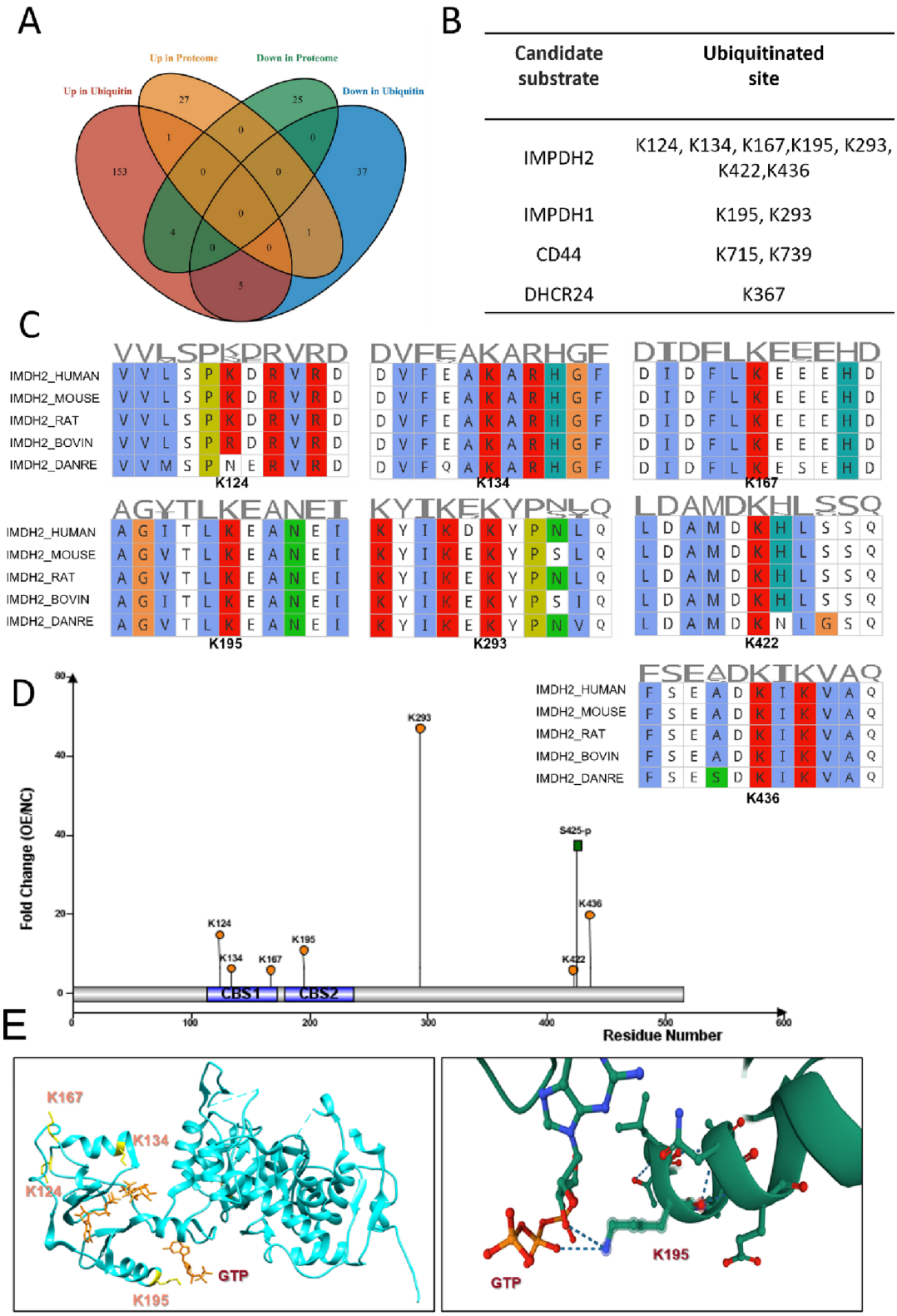

Figure 5. Integrative analysis of proteome and ubiquitinome. (A) Venn diagram showing the overlapping groups of proteins among differential regulated proteins and proteins with up- or down-regulated ubiquitylated lysine sites, OE cells versus NC cells. (B) A summary table showing that the candidate substrates of BTBD9 and their differential modified lysines were listed. (C) Bioinformatic alignment result of IMPDH2 in distinct species. (D) Pattern diagram displaying the location of differential ubiquitylated sites on IMPDH2. (E) 3D structure of IMPDH2 showing the distribution of ubiquitylated lysine.

BTBD9 overexpression cells, we carried out quality control analysis. The correlation analysis showed that both of the correlation coefficients between two groups were greater than 0.99, indicating good reproducibility within the groups (Figure 4A). Overall, 4635 proteins were identified in this analysis, and 3756 proteins were identified in both groups. By using a FC =

https://doi.org/10.1021/acsomega.1c07262
ACS Omega 2022, 7, 11839−11852

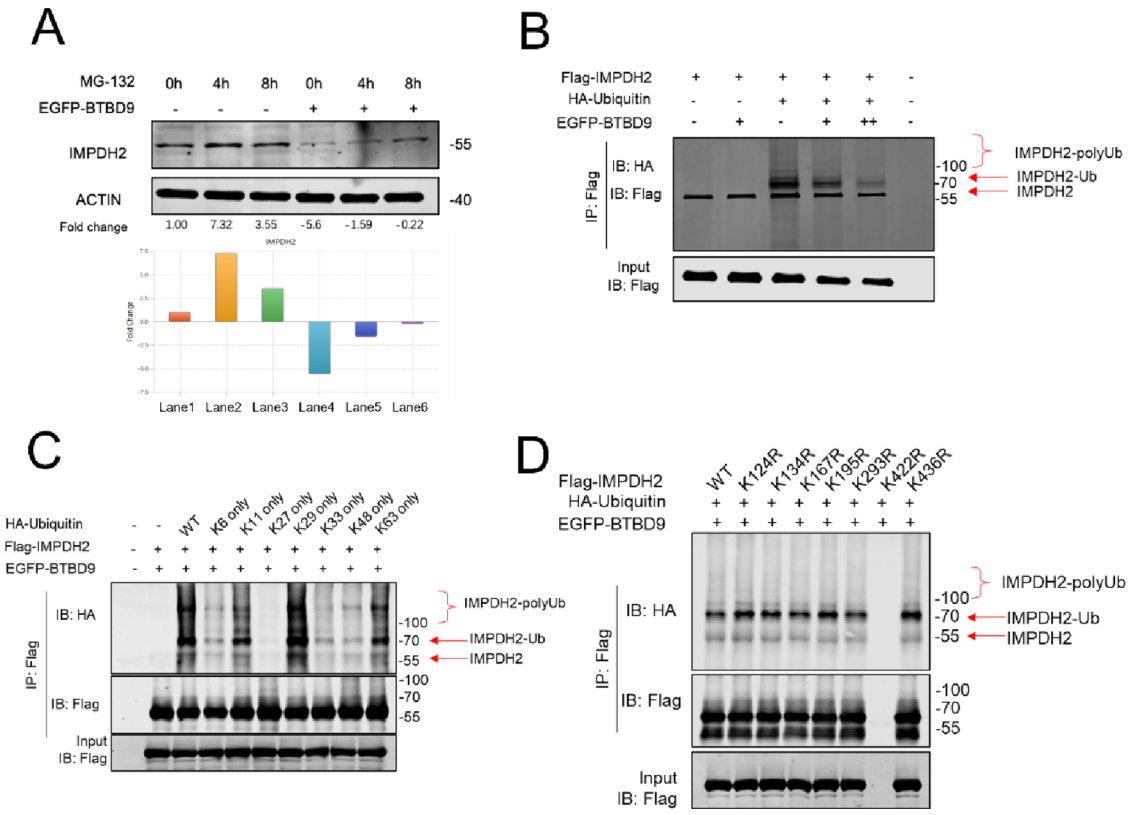

Figure 6. BTBD9 promotes IMPDH2 degradation. (A) Abundance of IMPDH2 under the treatment of MG132 by 4/8 h in NC cells and OE cells, respectively (fold change was calculated by Empiria Studio Software v1.3.0.83, File S1). (B) Immunoprecipitation result showing the influence of BTBD9 on ubiquitination modification of IMPDH2. (C) Immunoprecipitation result showing the ubiquitination mode of IMPDH2 by co-transfer 3× FLAG tagged IMPDH2 with distinct lysine mutant (L > R) ubiquitin. (D) Immunoprecipitation result showing the ubiquitination mode of IMPDH2 by co-transfer ubiquitin with distinct lysine mutant (L > R) IMPDH2.

1.2 and $P < 0.05$ as the differential expression threshold, we found that the expression of 29 proteins was up-regulated and that the expression of 29 proteins was down-regulated in *BTBD9* OE cells compared with NC cells (Figure 4B). The heatmap shows that the change in the expression of the differentially expressed genes was consistent in replicate samples (Figure 4C).

Gene set enrichment analysis (GSEA) was performed to analyze all significantly differentially expressed proteins (defined by a p value < 0.05) because the differentially expressed proteins were not suitable for over representation analysis (ORA) due to the limited number. The results showed that the differentially expressed genes were enriched in five categories of biological processes, including "vascular transport", "co-translational protein targeting to membrane", "protein targeting to membrane", and "import across plasma membrane" (Figure 4D). Of note, all these terms are related to protein transport, which is consistent with the results of ubiquitinome analysis and were all enriched for down-regulated genes. In addition, KEGG pathway analysis by GSEA revealed that two pathways were enriched after *BTBD9* overexpression: "Parkinson's disease" and the "ribosome pathway" (Figure 4E).

3.5. Identification of Candidate Substrates of BTBD9 for Degradation by Integrative Analysis. To identify the substrate that is specifically ubiquitinated by BTBD9, the proteomic and ubiquitinome profiling results were subjected to integrative analysis. Through this analysis, we identified six common proteins in both profiles (Figure 5A) and found that four of these proteins, i.e., inosine monophosphate dehydrogenase 1 (IMPDH1), inosine monophosphate dehydrogenase 1 (IMPDH2), CD44, and 24-dehydrocholesterol reductase (DHCR24), exhibited decreased protein expression and increased ubiquitination after *BTBD9* overexpression (Figure 5B). Considering that ubiquitinated proteins can be degraded by the proteasome, these four proteins were candidate targets of BTBD9-mediated ubiquitination. Among these four potential targets, IMPDH1 and IMPDH2 are isozymes that catalyze the conversion of inosine 5′-phosphate (IMP) to xanthosine 5′-phosphate (XMP), and they share 96.5% similarity in their amino acid sequences. Furthermore, the K195 and K293 residues of both IMPDH1 and IMPDH2 were ubiquitinated (Figure 5B), suggesting that these are the preferred residues of BTBD9-mediated ubiquitination.

Previous studies have suggested that *IMPDH1* and *IMPDH2* are circadian oscillators and that IMPDH2 is a preferred acetylation target of CLOCK.[30] Considering this finding, we hypothesized that *IMPDH2* has a potential role in sleep regulation; therefore, we chose this protein for the subsequent validation step. We identified seven ubiquitinated lysine residues in IMPDH2: K124, K134, K167, K195, K293, K422, and K436. Bioinformatic alignment showed that all of these ubiquitinated lysines are conserved among various species (Figure 5C). Analysis of IMPDH2 structure data showed that K124, K134, K167, and K195 are located in the cystathionine β-synthase (CBS) domain[31] (Figure 5D), which catalyzes the conversion of IMP to AMP.[32] Furthermore, K195 is required for the binding of the CBS domain to the allosteric effectors ATP and GTP (Figure 5E).

https://doi.org/10.1021/acsomega.1c07262
ACS Omega 2022, 7, 11839−11852

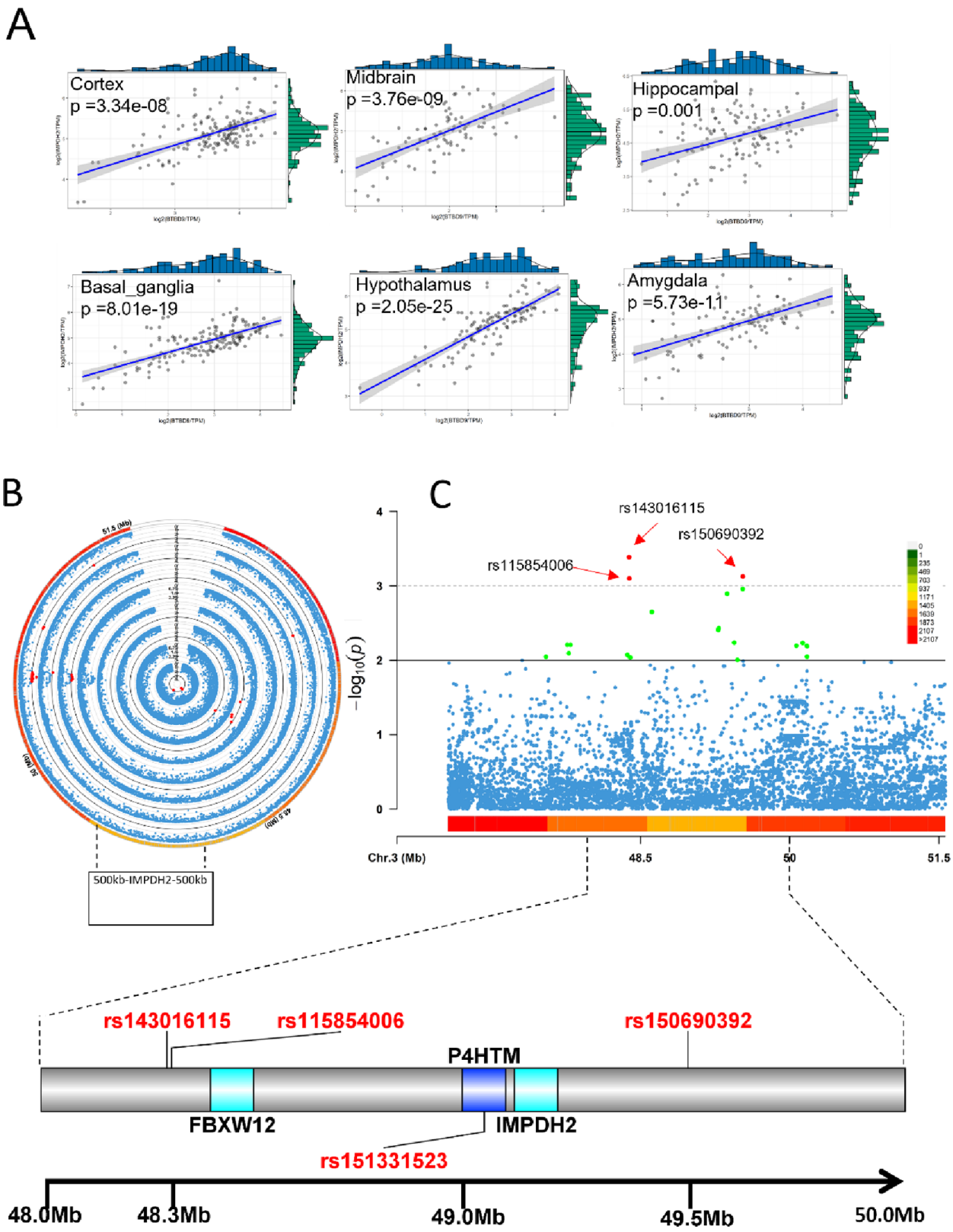

Figure 7. IMPDH2 is a potential target of BTBD9 in sleep regulation. (A) Scatter chart showing the correlation analysis result of BTBD9 expression and IMPDH2 expression in distinct brain area (cortex, midbrain, hippocampal, basal ganglia, hypothalamus, and amygdala). (B) Circular Manhattan plot GWAS showing the association of SNPs 2MB up- and downstream of IMPDH2 with sleep traits (N1/TST, N2/TST, N3/TST, WK/SPT, TST, and SE from innermost to outside). (C) Manhattan plot showing the association of SNPs related to N1/TST ($p < 10^{-3}$).

3.6. BTBD9 Promotes IMPDH2 Degradation. To validate whether BTBD9 regulates IMPDH2 degradation via ubiquitination, we treated NC and OE cells with the proteasome inhibitor MG132 and then examined the expression level of IMPDH2. The results showed that the protein expression of IMPDH2 was dramatically reduced in *BTBD9* OE cells and

https://doi.org/10.1021/acsomega.1c07262
ACS Omega 2022, 7, 11839−11852

greatly restored by the addition of MG132 (Figure 6A), indicating that the stability of IMPDH2 was regulated by the proteasome and that BTBD9 promoted this degradation. To further determine whether BTBD9 promotes IMPDH2 proteasome degradation through ubiquitination modification, *BTBD9* OE cells and NC cells were transfected with 3× FLAG-tagged IMPDH2 and HA-Ub and then treated with MG132 for 12 h before being collected. By using immunoprecipitation (IP), we surprisingly found that the overexpression of *BTBD9* decreased the ubiquitination of IMPDH2 (Figure 6B). This result is not in agreement with the results of our omics research. To determine why this phenomenon occurred, we carried out in vivo ubiquitination assays. The results showed that IMPDH2 was mainly ubiquitinated at K11, K29, and K63 rather than K48, which is the most common ubiquitination code that leads to UPS-mediated degradation[33] (Figure 6C). This result was validated by three independent experiments. We suspect that the suppression of the proteasome causes enhanced deubiquitylation activity that results in decreased ubiquitination of IMPDH2. To further clarify the ubiquitination mode of IMPDH2 by BTBD9, we constructed a 3× FLAG-tagged IMPDH2 plasmid with mutations of the significantly differentially modified sites and co-transfected cells with this plasmid in combination with a ubiquitin plasmid. The IP results demonstrated that there was little difference in the ubiquitination statues of IMPDH2 proteins with different lysine mutations, and to our surprise, IMPDH2 with a mutation at lysine K422 was not expressed in our study (Figure 6D).

3.7. IMPDH2 is a Potential Target of BTBD9 in Sleep Regulation. It has been proposed that homeostatic sleep factors act on brain regions and neurons involved in the regulation of sleep or wakefulness.[34] We first obtained expression data for *BTBD9* and *IMPDH2* in distinct brain regions from the GTEx database and performed a correlation analysis. The results showed that there was a significant positive correlation between the expression of *BTBD9* and *IMPDH2* in regions with high *BTBD9* expression, such as the hippocampus, and in several sleep regulation-related areas, such as the midbrain, hypothalamus, and basal ganglia (Figure 7A). This result suggested that *BTBD9* and *IMPDH2* may participate in some biological functions in a coordinated manner.

Next, to test whether *IMPDH2* is a potential regulator of sleep architecture, we used GWAS data to explore the association between genetic variations in *IMPDH2* and sleep parameters. The GWAS results showed that no SNPs of *IMPDH2* reached locus-wide significance ($P < 10^{-5}$). We next set a higher threshold for significance ($P < 10^{-3}$), and three SNPs were found to be associated with N1/TST (Figure 7B). These SNPs were rs143016112 (β = 1.01, se = 0.28, p = 0.00041), rs150690392 (β = 0.76, se = 0.23, p = 0.0008), and rs115854006 (β = 0.95, se = 0.28, p = 0.0008), which are between 48.0 and 50.0 Mbp of chromosome 3. This range includes much more than a 2 kb sequence upstream and downstream of *IMPDH2* (Figure 7C). Although none of the SNPs were reported to directly interact with *IMPDH2*, further analysis revealed that the intronic SNP rs151331523 of *P4HTM* (prolyl 4-hydroxylase, transmembrane (endoplasmic reticulum)) was in linkage disequilibrium with rs150690392 (r^2 = 0.98), and data from 3DSNP (http://cbportal.org/3dsnp/) suggest that this SNP interacts with the *IMPDH2* gene[35] (Figure S1). Altogether, these data suggest that IMPDH2 is a potential target for sleep regulation.

4. DISCUSSION

BTBD9 has been identified as a sleep regulation gene in several genetic studies, but its downstream targets and the molecular mechanisms through which it is involved in sleep regulation remain unclear. Our study revealed that the overexpression of the BTBD9 protein significantly, as an adaptive component of CRL3,[10] enhanced the ubiquitination of intracellular proteins and identified unique cellular pathways associated with these changes through quantitative ubiquitinome profiling. Ubiquitinome profiling combined with quantitative proteomics identified IMPDH2 as a novel substrate for BTBD9-mediated ubiquitination, which was confirmed by in vivo protein ubiquitination assays.

The role of *BTBD9* in sleep regulation has been validated by several studies on *BTBD9*-deficient animals, but most of the downstream targets of BTBD9 have been identified based on the mechanisms of restless leg syndrome, such as DNM1[14] and IRP2;[36] therefore, objective and comprehensive studies of the downstream targets of BTBD9 are lacking. In contrast, our study is the first to systematically explore the targets of BTBD9 through proteomic and ubiquitinome studies. First, we found that BTBD9 significantly enhanced ubiquitination in cells, suggesting that it has several ubiquitination targets. This is consistent with the finding of the current study, showing that thousands of proteins can be ubiquitinated, but only approximately 600 CRLs have been found.[7] However, the proteomic results suggest that BTBD9 has a slight effect on protein expression, suggesting that BTBD9 may be necessary for the normal function or localization of different ubiquitinated proteins rather than for the degradation of these proteins. This result is similar to the findings of quantitative phosphoproteomic studies of sleep-requiring substrates, showing that PTMs are also essential for sleep control but that protein abundance is unchanged.[37] On the other hand, enrichment analysis in both analyses showed that BTBD9 plays an important role in protein transport, especially in membrane structures, and down-regulates the expression of membrane proteins such as ATP1A1 and ATP1B1. Since previous studies have highlighted the important role of ion channels in sleep regulation[38,39] and Atp2b3 knockout mice have been reported to show increased sleep durations,[40] we hypothesized that BTBD9 may affect sleep homeostasis through ion metabolism, which may be mediated through regulation of protein localization. Furthermore, we identified IMPDH2 as a novel specific target whose stability is affected by BTBD9-mediated ubiquitination as IMPDH2 showed the most pronounced changes in both the proteomic and ubiquitinome studies. Furthermore, we found that the ubiquitination modifications of IMPDH2 are mainly K11-, K29-, and K63-dependent, but not the common K48 ubiquitination modifications. As a matter of fact, K11 and K29, the non-classical ubiquitination modification mode, have been shown to play a role in the proteasomal degradation pathway.[41,42] In contrast, K63 ubiquitination modifications are the most widely studied ubiquitination modifications other than K48 and have been partially found to have a role in triggering lysosomal-dependent protein degradation in addition to mediating signaling transduction.[43] Considering the function of *IMPDH2* in adenosine metabolism,[32,44] we generated an alternative hypothesis that BTBD9 can alter the function and expression of IMPDH2, subsequently leading to arousal by promoting the activity of pro-wake neurons due to a decrease in adenosine levels.[45] A previous study has shown that glutamatergic neurons in the basal

https://doi.org/10.1021/acsomega.1c07262
ACS Omega 2022, 7, 11839−11852

forebrain are closely related to adenosine concentrations in the basal forebrain and that the disruption of these neurons leads to impaired sleep homeostasis regulation in mice,[46] and the results of analysis of IMPDH2 expression patterns in the brain further support our hypothesis. In addition, we performed a GWAS to explore the relationship between variants associated with IMPDH2 and sleep characteristics and found that an SNP that interacts with IMPDH2 may affect N1 sleep stages.

Although our study made important discoveries and led to a hypothesis about the mechanism by which how *BTBD9* regulates sleep, there are some limitations. First, we chose cell lines as our research subject because they exhibit conserved biological function, thus allowing better extrapolation. However, brain tissues from *BTBD9*-deficient animals may better reflect the specific physiological process of sleep regulation. Second, only the interaction between IMPDH2 and BTBD9 was analyzed in this study. Although data from previous studies validated the association between these proteins in sleep-regulating brain areas, the role of IMPDH2 in sleep regulation needs to be further validated in animal models. Third, our GWAS data did not provide convincing results regarding the effect of IMPDH2 on sleep due to the small sample size. The use of a larger cohort may address this problem.

In summary, we comprehensively revealed the changes in ubiquitination mediated by BTBD9 and identified a novel target of BTBD9 with a potential role in sleep regulation; however, evidence from animal models supporting our hypothesis is still lacking. Given the numerous medical developments related to IMPDH2, once the role of IMPDH2 in sleep regulation is validated, targeting this protein may be greatly beneficial for the treatment of sleep diseases.

■ DECLARATION OF INTERESTS

■ ASSOCIATED CONTENT

Supporting Information

The Supporting Information is available free of charge at https://pubs.acs.org/doi/10.1021/acsomega.1c07262.

Figure S1. Circular plot of chromatin loops, states, and signatures associated to rs151331523 (provided by 3DSNP) and File S1. Quantitative analysis report of the blot picture concerning Figure 6A generated by Empiria Studio Software v1.3.0.83 (PDF)

■ AUTHOR INFORMATION

Corresponding Authors

Jian Guan − *Department of Otolaryngology Head and Neck Surgery & Center of Sleep Medicine, Otolaryngology Institute of Shanghai Jiao Tong University, Shanghai Jiao Tong University Affiliated Sixth People's Hospital, Shanghai 200233, China; Shanghai Key Laboratory of Sleep Disordered Breathing, Shanghai 200233, China*; Email: guanjian0606@sina.com

Feng Liu − *Department of Otolaryngology Head and Neck Surgery & Center of Sleep Medicine, Otolaryngology Institute of Shanghai Jiao Tong University, Shanghai Jiao Tong University Affiliated Sixth People's Hospital, Shanghai 200233, China; Shanghai Key Laboratory of Sleep Disordered Breathing, Shanghai 200233, China*; orcid.org/0000-0002-4442-7028; Email: liufeng@sibs.ac.cn

Shankai Yin − *Department of Otolaryngology Head and Neck Surgery & Center of Sleep Medicine, Otolaryngology Institute of Shanghai Jiao Tong University, Shanghai Jiao Tong University Affiliated Sixth People's Hospital, Shanghai 200233, China; Shanghai Key Laboratory of Sleep Disordered Breathing, Shanghai 200233, China*; Email: yinshankai@china.com

Authors

Zhenfei Gao − *Department of Otolaryngology Head and Neck Surgery & Center of Sleep Medicine, Otolaryngology Institute of Shanghai Jiao Tong University, Shanghai Jiao Tong University Affiliated Sixth People's Hospital, Shanghai 200233, China; Shanghai Key Laboratory of Sleep Disordered Breathing, Shanghai 200233, China*; orcid.org/0000-0002-0949-5084

Anzhao Wang − *Department of Otolaryngology Head and Neck Surgery & Center of Sleep Medicine, Otolaryngology Institute of Shanghai Jiao Tong University, Shanghai Jiao Tong University Affiliated Sixth People's Hospital, Shanghai 200233, China; Shanghai Key Laboratory of Sleep Disordered Breathing, Shanghai 200233, China*

Yongxu Zhao − *CAS Key Laboratory of Nutrition, Metabolism and Food Safety, Shanghai Institute of Nutrition and Health, Shanghai Institutes for Biological Sciences, University of Chinese Academy of Sciences, Chinese Academy of Sciences, Shanghai 200231, China*

Xiaoxu Zhang − *Department of Otolaryngology Head and Neck Surgery & Center of Sleep Medicine, Otolaryngology Institute of Shanghai Jiao Tong University, Shanghai Jiao Tong University Affiliated Sixth People's Hospital, Shanghai 200233, China; Shanghai Key Laboratory of Sleep Disordered Breathing, Shanghai 200233, China*

Xiangshan Yuan − *Department of Anatomy and Histoembryology, School of Basic Medical Sciences, State Key Laboratory of Medical Neurobiology and MOE Frontiers Center for Brain Science, Institutes of Brain Science, Fudan University, Shanghai 200231, China*

Niannian Li − *Department of Otolaryngology Head and Neck Surgery & Center of Sleep Medicine, Otolaryngology Institute of Shanghai Jiao Tong University, Shanghai Jiao Tong University Affiliated Sixth People's Hospital, Shanghai 200233, China; Shanghai Key Laboratory of Sleep Disordered Breathing, Shanghai 200233, China*

Chong Xu − *Department of Otolaryngology Head and Neck Surgery & Center of Sleep Medicine, Otolaryngology Institute of Shanghai Jiao Tong University, Shanghai Jiao Tong University Affiliated Sixth People's Hospital, Shanghai 200233, China; Shanghai Key Laboratory of Sleep Disordered Breathing, Shanghai 200233, China*

Shenming Wang − *Department of Otolaryngology Head and Neck Surgery & Center of Sleep Medicine, Otolaryngology Institute of Shanghai Jiao Tong University, Shanghai Jiao Tong University Affiliated Sixth People's Hospital, Shanghai 200233, China; Shanghai Key Laboratory of Sleep Disordered Breathing, Shanghai 200233, China*

Yaxin Zhu − *Department of Otolaryngology Head and Neck Surgery & Center of Sleep Medicine, Otolaryngology Institute of Shanghai Jiao Tong University, Shanghai Jiao Tong University Affiliated Sixth People's Hospital, Shanghai 200233, China; Shanghai Key Laboratory of Sleep Disordered Breathing, Shanghai 200233, China*

Jingyu Zhu − *Department of Otolaryngology Head and Neck Surgery & Center of Sleep Medicine, Otolaryngology Institute of Shanghai Jiao Tong University, Shanghai Jiao Tong*

University Affiliated Sixth People's Hospital, Shanghai 200233, China; Shanghai Key Laboratory of Sleep Disordered Breathing, Shanghai 200233, China

Complete contact information is available at:
https://pubs.acs.org/10.1021/acsomega.1c07262

Author Contributions

[#]Z.G. and A.W. contributed equally to this work. F.L., J.G., and S.Y. conceived the present idea of this study. Y.Z. and X.Z. helped to validate the result of proteomics. N.L., S.W., X.Z., J.Z., and Y.Z. were all involved in data processing. Z.G. was responsible for writing the manuscript, and F.L. revised this manuscript. All the authors have read and approved the final manuscript.

Funding

This study was supported by the National Science Foundation (no. 81971240 to F.L., 81970870 to J.G.), Shanghai Municipal Commission of Science and Technology (no. 18DZ2260200), and Shanghai Municipal Education Commission (2017-01-07-00-02-E00047).

Notes

The authors declare no competing financial interest.
The data that support the findings of this study are available from the corresponding author upon reasonable request.

■ ACKNOWLEDGMENTS

We deeply thank Dr. Xiangshan Yuan (Department of Pharmacology, Fudan University, Shanghai, China) for helping us with the EEG/EMG implantation surgery and data analysis for sleep parameters. The gene expression data used for the analyses described in this manuscript were obtained from the GTEx Portal.

■ REFERENCES

(1) Rape, M. Ubiquitylation at the crossroads of development and disease. *Nat. Rev. Mol. Cell Biol.* **2018**, *19*, 59−70.
(2) Popovic, D.; Vucic, D.; Dikic, I. Ubiquitination in disease pathogenesis and treatment. *Nat. Med.* **2014**, *20*, 1242−1253.
(3) Kikuma, K.; Li, X.; Perry, S.; Li, Q.; Goel, P.; Chen, C.; Kim, D.; Stavropoulos, N.; Dickman, D. Cul3 and insomniac are required for rapid ubiquitination of postsynaptic targets and retrograde homeostatic signaling. *Nat. Commun.* **2019**, *10*, 2998.
(4) Lane, J. M.; Jones, S. E.; Dashti, H. S.; Wood, A. R.; Aragam, K. G.; van Hees, V. T.; Strand, L. B.; Winsvold, B. S.; Wang, H.; Bowden, J.; et al. Biological and clinical insights from genetics of insomnia symptoms. *Nat. Genet.* **2019**, *51*, 387−393.
(5) Pickart, C. M. Mechanisms underlying ubiquitination. *Annu. Rev. Biochem.* **2001**, *70*, 503−533.
(6) Zheng, N.; Shabek, N. Ubiquitin Ligases: Structure, Function, and Regulation. *Annu. Rev. Biochem.* **2017**, *86*, 129−157.
(7) Sarikas, A.; Hartmann, T.; Pan, Z.-Q. The cullin protein family. *Genome Biol.* **2011**, *12*, 220.
(8) Freeman, A. A. H.; Mandilaras, K.; Missirlis, F.; Sanyal, S. An emerging role for Cullin-3 mediated ubiquitination in sleep and circadian rhythm: insights from Drosophila. *Fly* **2013**, *7*, 39−43.
(9) Stavropoulos, N.; Young, M. W. insomniac and Cullin-3 regulate sleep and wakefulness in Drosophila. *Neuron* **2011**, *72*, 964−976.
(10) Stogios, P. J.; Downs, G. S.; Jauhal, J. J. S.; Nandra, S. K.; Privé, G. G. Sequence and structural analysis of BTB domain proteins. *Genome Biol.* **2005**, *6*, R82.
(11) Stefansson, H.; Rye, D. B.; Hicks, A.; Petursson, H.; Ingason, A.; Thorgeirsson, T. E.; Palsson, S.; Sigmundsson, T.; Sigurdsson, A. P.; Eiriksdottir, I.; et al. A genetic risk factor for periodic limb movements in sleep. *N Engl J Med.* **2007**, *357*, 639−647.
(12) Winkelmann, J.; Schormair, B.; Lichtner, P.; Ripke, S.; Xiong, L.; Jalilzadeh, S.; Fulda, S.; Pütz, B.; Eckstein, G.; Hauk, S.; et al. Genome-wide association study of restless legs syndrome identifies common variants in three genomic regions. *Nat. Genet.* **2007**, *39*, 1000−1006.
(13) DeAndrade, M. P.; Johnson, R. L., Jr.; Unger, E. L.; Zhang, L.; van Groen, T.; Gamble, K. L.; Li, Y. Motor restlessness, sleep disturbances, thermal sensory alterations and elevated serum iron levels in Btbd9 mutant mice. *Hum. Mol. Genet.* **2012**, *21*, 3984−3992.
(14) Freeman, A.; Pranski, E.; Miller, R. D.; Radmard, S.; Bernhard, D.; Jinnah, H. A.; Betarbet, R.; Rye, D. B.; Sanyal, S. Sleep fragmentation and motor restlessness in a Drosophila model of Restless Legs Syndrome. *Curr. Biol.* **2012**, *22*, 1142−1148.
(15) Grima, B.; Dognon, A.; Lamouroux, A.; Chélot, E.; Rouyer, F. CULLIN-3 controls TIMELESS oscillations in the Drosophila circadian clock. *PLoS Biol.* **2012**, *10*, No. e1001367.
(16) Shen, Y.; Yu, W.-B.; Shen, B.; Dong, H.; Zhao, J.; Tang, Y.-L.; Fan, Y.; Yang, Y.-F.; Sun, Y.-M.; Luo, S.-S.; et al. Propagated α-synucleinopathy recapitulates REM sleep behaviour disorder followed by parkinsonian phenotypes in mice. *Brain.* **2020**, *143*, 3374−3392.
(17) Mi, H.; Muruganujan, A.; Ebert, D.; Huang, X.; Thomas, P. D. PANTHER version 14: more genomes, a new PANTHER GO-slim and improvements in enrichment analysis tools. *Nucleic Acids Res.* **2019**, *47*, D419−D426.
(18) Kanehisa, M.; Goto, S. KEGG: kyoto encyclopedia of genes and genomes. *Nucleic Acids Res.* **2000**, *28*, 27−30.
(19) Blum, M.; Chang, H. Y.; Chuguransky, S.; Grego, T.; Kandasaamy, S.; Mitchell, A.; Nuka, G.; Paysan-Lafosse, T.; Qureshi, M.; Raj, S.; et al. The InterPro protein families and domains database: 20 years on. *Nucleic Acids Res.* **2021**, *49*, D344−D354.
(20) Yu, G.; Wang, L.-G.; Han, Y.; He, Q.-Y. clusterProfiler: an R package for comparing biological themes among gene clusters. *OMICS* **2012**, *16*, 284−287.
(21) Subramanian, A.; Tamayo, P.; Mootha, V. K.; Mukherjee, S.; Ebert, B. L.; Gillette, M. A.; Paulovich, A.; Pomeroy, S. L.; Golub, T. R.; Lander, E. S.; Mesirov, J. P. Gene set enrichment analysis: a knowledge-based approach for interpreting genome-wide expression profiles. *Proc. Natl. Acad. Sci. U. S. A.* **2005**, *102*, 15545−15550.
(22) Tuefferd, M.; De Bondt, A.; Van Den Wyngaert, I.; Talloen, W.; Verbeke, T.; Carvalho, B.; Clevert, D. A.; Alifano, M.; Raghavan, N.; Amaratunga, D.; et al. Genome-wide copy number alterations detection in fresh frozen and matched FFPE samples using SNP 6.0 arrays. *Genes, Chromosomes Cancer* **2008**, *47*, 957−964.
(23) Yin, L.; Zhang, H.; Tang, Z.; Xu, J.; Yin, D.; Zhang, Z.; Yuan, X.; Zhu, M.; Zhao, S.; Li, X.; et al. rMVP: A Memory-efficient, Visualization-enhanced, and Parallel-accelerated tool for Genome-Wide Association Study. *Genomics Proteomics Bioinformatics.* **2021**, DOI: 10.1016/j.gpb.2020.10.007.
(24) Gibson, G. Hints of hidden heritability in GWAS. *Nat. Genet.* **2010**, *42*, 558−560.
(25) Xicoy, H.; Wieringa, B.; Martens, G. J. M. The SH-SY5Y cell line in Parkinson's disease research: a systematic review. *Mol Neurodegener.* **2017**, *12*, 10.
(26) Li, L.; Zhang, W.; Liu, Y.; Liu, X.; Cai, L.; Kang, J.; Zhang, Y.; Chen, W.; Dong, C.; Zhang, Y.; Wang, M.; Wei, W.; Jia, L. The CRL3(BTBD9) E3 ubiquitin ligase complex targets TNFAIP1 for degradation to suppress cancer cell migration. *Signal Transduction Targeted Ther.* **2020**, *5*, 42.
(27) Chou, M. F.; Schwartz, D. Biological sequence motif discovery using motif-x. *Curr. Protoc. Bioinf.* **2011**, *13*, 15−24.
(28) Kastenhuber, E. R.; Lowe, S. W. Putting p53 in Context. *Cell* **2017**, *170*, 1062−1078.
(29) Janke, C.; Magiera, M. M. The tubulin code and its role in controlling microtubule properties and functions. *Nat Rev Mol Cell Biol.* **2020**, *21*, 307−326.
(30) Lin, R.; Mo, Y.; Zha, H.; Qu, Z.; Xie, P.; Zhu, Z.-J.; Xu, Y.; Xiong, Y.; Guan, K.-L. CLOCK Acetylates ASS1 to Drive Circadian Rhythm of Ureagenesis. *Mol. Cell* **2017**, *68*, 198.
(31) Ren, J.; Wen, L.; Gao, X.; Jin, C.; Xue, Y.; Yao, X. DOG 1.0: illustrator of protein domain structures. *Cell Res.* **2009**, *19*, 271−273.

(32) Baykov, A. A.; Tuominen, H. K.; Lahti, R. The CBS domain: a protein module with an emerging prominent role in regulation. *ACS Chem. Biol.* **2011**, *6*, 1156−1163.
(33) Tracz, M.; Bialek, W. Beyond K48 and K63: non-canonical protein ubiquitination. *Cell Mol Biol Lett.* **2021**, *26*, 1.
(34) Brown, R. E.; Basheer, R.; McKenna, J. T.; Strecker, R. E.; McCarley, R. W. Control of sleep and wakefulness. *Physiol Rev.* **2012**, *92*, 1087−1187.
(35) Lu, Y.; Quan, C.; Chen, H.; Bo, X.; Zhang, C. 3DSNP: a database for linking human noncoding SNPs to their three-dimensional interacting genes. *Nucleic Acids Res.* **2016**, *45*, D643−D649.
(36) DeAndrade, M. P.; Zhang, L.; Doroodchi, A.; Yokoi, F.; Cheetham, C. C.; Chen, H. X.; Roper, S. N.; Sweatt, J. D.; Li, Y. Enhanced hippocampal long-term potentiation and fear memory in Btbd9 mutant mice. *PLoS One* **2012**, *7*, No. e35518.
(37) Wang, Z.; Ma, J.; Miyoshi, C.; Li, Y.; Sato, M.; Ogawa, Y.; Lou, T.; Ma, C.; Gao, X.; Lee, C.; et al. Quantitative phosphoproteomic analysis of the molecular substrates of sleep need. *Nature* **2018**, *558*, 435−439.
(38) Ingiosi, A. M.; Hayworth, C. R.; Harvey, D. O.; Singletary, K. G.; Rempe, M. J.; Wisor, J. P.; Frank, M. G. A Role for Astroglial Calcium in Mammalian Sleep and Sleep Regulation. *Curr. Biol.* **2020**, *30*, 4373−4383.e7 e4377.
(39) Liu, S.; Liu, Q.; Tabuchi, M.; Wu, M. N. Sleep Drive Is Encoded by Neural Plastic Changes in a Dedicated Circuit. *Cell* **2016**, *165*, 1347−1360.
(40) Tatsuki, F.; Sunagawa, G. A.; Shi, S.; Susaki, E. A.; Yukinaga, H.; Perrin, D.; Sumiyama, K.; Ukai-Tadenuma, M.; Fujishima, H.; Ohno, R.; Tone, D.; Ode, K. L.; Matsumoto, K.; Ueda, H. R. Involvement of Ca(2+)-Dependent Hyperpolarization in Sleep Duration in Mammals. *Neuron* **2016**, *90*, 70−85.
(41) Komander, D.; Rape, M. The ubiquitin code. *Annu. Rev. Biochem.* **2012**, *81*, 203−229.
(42) Swatek, K. N.; Komander, D. Ubiquitin modifications. *Cell Res.* **2016**, *26*, 399−422.
(43) Saeki, Y.; Kudo, T.; Sone, T.; Kikuchi, Y.; Yokosawa, H.; Toh-e, A.; Tanaka, K. Lysine 63-linked polyubiquitin chain may serve as a targeting signal for the 26S proteasome. *EMBO J.* **2009**, *28*, 359−371.
(44) Pimkin, M.; Pimkina, J.; Markham, G. D. A regulatory role of the Bateman domain of IMP dehydrogenase in adenylate nucleotide biosynthesis. *J Biol Chem.* **2009**, *284*, 7960−7969.
(45) Thakkar, M. M.; Delgiacco, R. A.; Strecker, R. E.; McCarley, R. W. Adenosinergic inhibition of basal forebrain wakefulness-active neurons: a simultaneous unit recording and microdialysis study in freely behaving cats. *Neuroscience* **2003**, *122*, 1107−1113.
(46) Peng, W.; Wu, Z.; Song, K.; Zhang, S.; Li, Y.; Xu, M. Regulation of sleep homeostasis mediator adenosine by basal forebrain glutamatergic neurons. *Science* **2020**, *369*, eabb0556s.

https://doi.org/10.1021/acsomega.1c07262
ACS Omega 2022, 7, 11839−11852